

# Assessment of Infant Brain Development With Frequency-Domain Near-Infrared Spectroscopy

MARIA ANGELA FRANCESCHINI, SONAL THAKER, GEORGE THEMELIS, KALPATHY K. KRISHNAMOORTHY, HEATHER BORTFELD, SOLOMON G. DIAMOND, DAVID A. BOAS, KARA ARVIN, AND P. ELLEN GRANT

*Athinoula A. Martinos Center [M.A.F., S.T., G.T., S.G.D., D.A.B., E.G.], Massachusetts General Hospital, Charlestown, Massachusetts 02129; Division of Pediatric Neurology K.K.K., Department of Neonatology [K.A.], Department of Radiology [E.G.], Massachusetts General Hospital, Boston, Massachusetts 02114; Department of Psychology [H.B.], Texas A&M University, College Station, Texas 77843*

**ABSTRACT:** This is the first report to demonstrate quantitative monitoring of infant brain development with frequency-domain near-infrared spectroscopy (FD-NIRS). Regionally specific increases in blood volume and oxygen consumption were measured in healthy infants during their first year. The results agree with prior PET and SPECT reports; but, unlike these methods, FD-NIRS is portable and uses nonionizing radiation. Further, new information includes the relatively constant tissue oxygenation with age and location, suggesting a tight control between local oxygen delivery and consumption in healthy infants during brain development. FD-NIRS could become the preferred clinical tool for quantitatively assessing infant brain development. (*Pediatr Res* 61: 546–551, 2007)

The rate of growth and development in the first year of life is unmatched at any other time during postnatal development (1). However, with rapid growth comes increased vulnerability to disorders arising from genetic defects, gene expression, and environmental exposures. Injuries or abnormal gene expressions occurring early in life are expected to have profound effects on neuronal organization and integrated neuronal activity as many axono-dendritic connections are formed and the majority of myelination occurs in the first year (2). Despite the high vulnerability in the first year, there are very few tools available for assessment of brain health and current clinical exams are notoriously insensitive. To better understand normal developmental trajectories and to distinguish abnormal from normal trajectories at an early time point, a safe, inexpensive, portable technique for quantitative, reliable monitoring of regional brain development is needed.

Current understandings of regional brain development in infants derive from PET and SPECT studies, with the inherent risk of radiation exposure, and from MRI studies, which, although safe, typically require sedation of infants more than a few weeks old to prevent movements during the scans. Most studies conducted with these techniques are in fact performed for other clinical indications with small populations of unhealthy infants. Using 2-deoxy-2-[<sup>18</sup>F]-fluoro-D-glucose PET,

Chugani and Phelps (3) has demonstrated a correlation between glucose utilization and behavioral and neurophysiological maturation. In newborns, glucose uptake is highest in the sensorimotor cortex, with generally low functional activity over most of the remaining cerebral cortex. During the second and third months, glucose uptake begins to increase in the parietal, temporal and primary visual cortices. This coincides with improvements in motor and visual skills at this age (4,5), as well as with changes in the EEG response to stimuli (6). Glucose uptake has increased in the lateral inferior frontal cortex by 6–8 mo, and by 12 mo in the dorsal and medial frontal cortex. At the same time, infants show improved cognitive and behavioral performance. By approximately 1 y of age, the pattern of glucose utilization in an infant resembles that of an adult (7). Other investigators have noted similar developmental changes in CBF using PET H<sub>2</sub> <sup>15</sup>O (8) and iodine-123 iodoamphetamine SPECT (9). The progression of myelination with age observed in a small number of infants undergoing MRI for clinical reasons has been described qualitatively (10,11). Regional myelination changes correlate with glucose uptake and increases in CBF (12). The exact cause of the higher blood flow observed in myelinating and myelinated brain regions is not known. However, increases in blood flow and glucose metabolism occur at about the same time, suggesting either higher energy demand during myelination or, more likely, increased cerebral activity in the myelinating regions.

Increases in capillary density support increases in blood flow, resulting in increased blood volume. Furthermore, such increases occur with and may slightly precede increases in glucose metabolism. NIRS provides bedside monitoring of cerebral blood volume and an alternative measure of cerebral metabolism: oxygen consumption. The method is rapid, portable, and noninvasive. More importantly, it is absolutely safe because it uses nonionizing radiation and deposits less energy than a cerebral ultrasound. Ethically, therefore, NIRS can be used to study brain development in healthy infants. NIRS was first applied to the study of neonates in the late 1970s to

Received August 25, 2006; accepted January 9, 2007.

Correspondence: Maria Angela Franceschini, Ph.D., Athinoula A. Martinos Center, Massachusetts General Hospital, 13th St, Building 149, Charlestown, Massachusetts 02129; e-mail: mari@nmr.mgh.harvard.edu

Supported by the U.S. National Institutes of Health grant no. RO1-HD42908 (MAF) and no. K23 NS42758 (PEG).

DOI: 10.1203/pdr.0b013e318045be99

**Abbreviations:** CBF, cerebral blood flow; CBV, cerebral blood volume; CMRO<sub>2</sub>, cerebral metabolic rate of oxygen; FD, frequency-domain; HbT, total hemoglobin concentration; HGB, hemoglobin concentration in the blood; NIRS, near-infrared spectroscopy StO<sub>2</sub>, tissue oxygen saturation

mid-1980s (13–15). Widespread adoption of this technology has been limited, though, by a lack of quantification (16) or by complexity of the imaging systems (17,18). Recent advances in technology and development of more sophisticated time- and frequency-domain (FD) systems have increased quantitative accuracy while maintaining simplicity (19,20).

We used a frequency-domain device (Imagent, ISS Inc., Champaign, IL), modified to have multiple source wavelengths and multiple detectors at varying distances. This multi-distance instrument allows us to quantify the optical properties of the examined tissue while making fewer assumptions than was necessary with previous systems (14,16). By simply holding the optical probe on an infant's head for few seconds, one can quantify regional tissue  $\text{StO}_2$ , HbT, and CBV, and provide estimates of relative changes in the  $\text{CMRO}_2$ . We measured six brain regions on 47 healthy infants and determined regional vascular and metabolic changes during development.

## METHODS

**Population and protocol.** We recruited 47 healthy infants ranging in age from premature to 12 mo of age. Thirty were males; the average gestational age (GA) at birth was 37.9 wk (27.0–41.5 wk GA). Twenty-eight normal infants, age 20–50 wk, were recruited in Texas (Department of Psychology, Texas A&M University). Eleven normal infants (*i.e.* carried to term) were recruited from the Well Baby Nursery at the Massachusetts General Hospital (MGH). Eight healthy preterm infants were recruited from the NICU or Step-Down Unit at the MGH. Preterm infants were considered normal if they had a normal head ultrasound, low risk for cerebral injury, no lung disease on the day of measurement, and normal blood gases and hematocrit values. Two infants were measured twice. Measurements for two infants were discarded because of poor data quality. Furthermore, we measured one healthy term infant multiple times from birth to 11 mo of age. The data from this infant are reported separately to demonstrate the statistical advantage of a longitudinal study. Informed consent was obtained from all parents. The protocol was approved by the local institutional review boards.

The protocol consisted of positioning the probe on six different regions of the head (frontal = fr, occipital = oc, left temporal = lt, left parietal = lp, right temporal = rt, and right parietal = rp cortices) and holding it in place for 8 s of data acquisition (Fig. 1). In 60% of the infants we acquired data on the six positions more than once during the same measurement session to evaluate reproducibility. In these cases, we repositioned

the probe in nearby positions to ensure that local inhomogeneities such as hair and superficial large vessels were not affecting the measurement, and that the measurement was representative of the underlying brain region. Repositioning the probe in neighboring locations but not in the exact location is the main reason we obtained larger reproducibility errors than have been previously published with NIRS (20), and this is due to the heterogeneity of the tissue, not to instrumental limits.

**Instrument.** We used a customized commercial frequency-domain oximeter (Imagent, ISS Inc.) with 32 laser sources and 4 photomultiplier tube detectors. The instrument is quite compact and can be moved on a small cart, for example, to the infant's bedside in the hospital. The sources are modulated at 110 MHz; the detectors at 110 MHz plus 5 kHz to achieve heterodyne detection. The lasers are rapidly multiplexed (10 ms) in sequence, so only one source is on at any given time, allowing separation by software on the detector side. The light power emitted by the lasers at the fiber end is  $<1$  mW in a 5 mm<sup>2</sup> area, well below the ANSI standard limits, allowing safe measurements. For these measurements we used seven lasers (emitting at 670, 690, 750, 760, 780, 810, and 830 nm) combined in a source fiber bundle, and four detectors coupled to four fiber bundles. The optical fibers were arranged in a row in a flexible black rubber probe (5 × 2 × 0.5 cm<sup>3</sup>) with source-detector distances of 1, 1.5, 2, and 2.5 cm. Multiple distances are necessary to quantify absorption and scattering coefficients with this system (21).

These source-detector separations are adequate for the population investigated (22,23). Larger separations would make the probe too large for premature, newborn babies, and for some locations in older children. We try to avoid bending the probe, which increases the error in the effective source-detector separations and affects calculation of optical properties. To confirm that the source-detector distances were sufficient for the photons to reach the brain cortex, we performed functional tests in the parietal and occipital regions in a 2-mo-old and a 4-mo-old infant; we obtained evoked hemodynamic responses at all distances (data not shown here). Nevertheless, we observed that in older children (2 mo or older) the values of the amplitude (root mean squared ac) and phase for the first source-detector separation were not always in line with the other three distances, probably because of the larger head size and more optically dense bone reducing the brain sensitivity of the 1 cm measurement. Similarly, in premature babies and in some head positions in older children, the fourth distance was not in line with the other three, because of poor contact resulting from the larger curvature in smaller heads. In these cases, we excluded one distance from the data analysis.

**Data analysis.** Absorption and reduced scattering coefficients at each wavelength were calculated from the amplitude and phase data using the multi-distance frequency-domain method (21). Because we separate absorption and scattering there is no need to assume a pathlength factor at each wavelength as is done with CW systems. Hb concentration and oxygenation were derived by fitting the absorption coefficient at seven wavelengths, with the Hb spectra using extinction

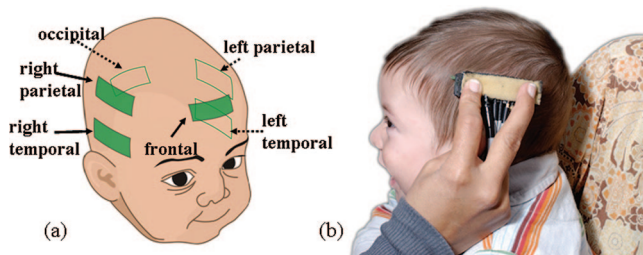


**Figure 1.** (a) Probe positions and (b) measurement of an infant.

coefficients reported in the literature (24). For this we developed a graphical interface program (GUI) implemented in MATLAB (The Mathworks, Inc., Natick, MA) with a quick visual display of the results (the program is available for free download at <http://www.nmr.mgh.harvard.edu/DOT/resources/FDMDGUI/>).

Cerebral blood volume was calculated using the following equation (19):

$$CBV = \frac{(HbT \times MW_{Hb})}{HGB \times D_{bt}}$$

CBV is in units of mL/100g,  $MW_{Hb} = 64,500$  [g/Mol] is the molecular weight of Hb and  $D_{bt}$  is the brain tissue density (1.05 g/mL) (1). HGB is the Hb concentration in the blood (g/dL). Measurements of HGB and hematocrit were available only for premature babies and two newborns. For the other infants we used standard normal values for HGB as a function of age, taken from the literature (25). While this increases variance in the population estimates, the variance is small when applied to the healthy subject.

We also calculated changes with age in the cerebral metabolic rate of oxygen. The  $\Delta CMRO_2$  calculation is based on the relation

$$CMRO_2 = \frac{HGB \cdot CBF \cdot (SaO_2 - SvO_2)}{MW_{hb}}$$

where CBF = cerebral blood flow and  $SaO_2$  = arterial and  $SvO_2$  = venous Hb oxygenation. Since we did not make direct measurements of CBF and  $SvO_2$ , we worked from the assumption that

$$StO_2 = aSaO_2 + bSvO_2$$

with  $a + b = 1$  and  $b$  constant with age (26). Next, we assumed a constant power law relation between changes in blood flow and blood volume with age

$$CBF/CBF = (CBV/CBV_o)^\beta$$

with  $2 \leq \beta \leq 3$  (27,28) and the subscript  $o$  indicating the initial measure. Finally, we obtain

$$\Delta CMRO_2 = \frac{CMRO_2}{CMRO_{2o}} = \frac{HGB}{HGB_o} \cdot \left(\frac{CBV}{CBV_o}\right)^\beta \cdot \left(\frac{SaO_2 - StO_2}{SaO_{2o} - StO_{2o}}\right)$$

**Uncertainties in physiologic parameters.** To quantify HbT, CBV, and  $\Delta CMRO_2$ , we assume known values for molecular weight of Hb, brain tissue density, Hb extension coefficients, and water concentration.

Molecular weight of Hb values reported in the literature varies between 62,000 and 65,000 D. In our calculations we used 64,500 D, which if inaccurate will result in a systematic error and influence the results all in the same way. More importantly,  $MW_{Hb}$  doesn't change with age and is the same for fetal and adult Hb (29).

The brain tissue density  $D_{bt}$  we used, 1.03 g/mL, is for adult brain, historically the value used also in the analysis of fetal specimens (1).

With the wavelengths used it is not possible to estimate water concentration, and we cannot add a wavelength closer to the water absorption peak (980 nm) because our detectors' sensitivity is effectively zero beyond 850 nm. We therefore

assumed a water concentration of 75% (30). Although the water concentration is higher in neonatal brains, it rapidly decreases over the first year as myelination occurs. Since variations of 10% in water concentration cause errors in HbT and  $StO_2$  of no larger than 3% and 2%, respectively, we elected to use the adult value instead of estimating water concentration at each age.

For Hb absorption we used the extinction coefficient of adult Hb found in the literature (24). We compared the published spectra of adult and fetal Hb (31) and saw no significant differences in the spectral range used.

Some NIRS groups use a cerebral to large vessel hematocrit ratio of 0.69 to correct for the fact the hematocrit in small vessels is lower than the hematocrit measured in large vessels with a blood test (32). We decided not to use this factor because values in adults reported in the literature vary from 0.69 (33) to 0.88 (34) and because it has never been measured in infants and may vary with age. Adding this 0.69 factor would increase CBV to 2.9 mL/100g in premature babies and 5.5 mL/100 g in 10–12-mo-old babies.

**Data selection.** Importantly, our FD-NIRS instrument employs seven instead of the typical two wavelengths necessary to quantify Hb properties. The redundancy offered by more wavelengths allows us to assess the quality of the measurements and objectively discard poor datasets, increasing the accuracy of our measures and decreasing contamination from noise. Poor quality data often arises from improper probe contact, hair obscuring the optical fibers, and laser light reaching the detectors without traversing through the tissue. We discarded all data with  $R^2 < 0.97$  for the model fit of the raw optical data,  $p$  values  $>0.05$  for the Hb spectral fit of the seven measured absorption coefficients, or  $p$  values  $>0.1$  for the linear fit of the reduced scattering coefficients versus wavelength.

This *ad hoc* data rejection criteria enabled us to remove all data that qualitatively appeared corrupted by measurement noise. Further studies are required to determine whether these criteria will become standardized in the processing stream. Presently, these criteria allowed us to assess the quality of the measurements systematically, to report our methodology objectively, and to reduce the variance in our results.

## RESULTS

Figure 2 shows the rates of growth per week from birth to 1 y of age for HbT, CBV, and  $StO_2$  measured across all babies; Figure 3 shows the measurements in the frontal region with the linear fits for this and other age ranges. The average rate of increase in HbT from birth to 1 y of age is 0.5  $\mu$ M per week, and for CBV 0.036 mL/100 g per week. On average, HbT increases 50% and CBV 84% between 0 and 50 wk. In contrast, the average rate of  $StO_2$  increase is not significant in all brain regions, with only 2% change between 0 and 50 wk. On average  $StO_2$  is 64% ( $\pm 5\%$  SD) across all brain regions and ages. Sorting the infants by corrected gestational age (cGA) instead of chronological age yields slightly weaker linear correlations for CBV, but slightly stronger correlations for HbT.



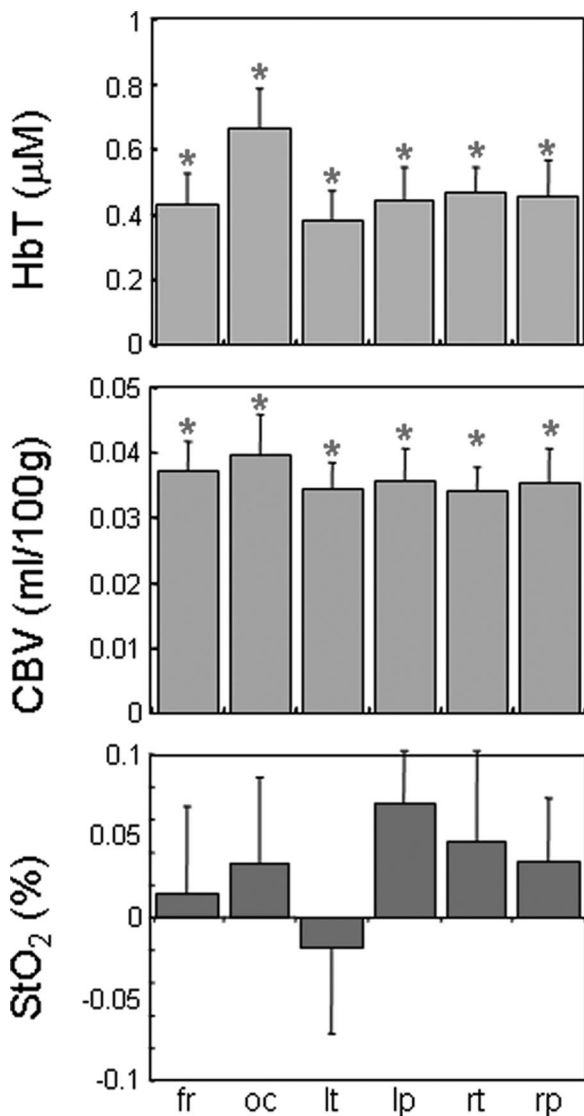


**Figure 2.** Linear per week changes in HbT (*top*), CBV (*middle*), and StO<sub>2</sub> (*bottom*) from 0 to 50 wk in six brain regions. \* $p < 0.05$ . The error bars are SD. The numbers of subjects for the six locations are: 35, 35, 38, 43, 38, and 39.

We divided the data into two age intervals (0–6 wk and 12–50 wk) corresponding to two different hemodynamic behaviors. From 0 to 6 wk we observed a significant decrease in HbT and StO<sub>2</sub> with CBV relatively constant in all regions measured. From 12 to 50 wk, we found statistically significant increases in HbT, CBV, and StO<sub>2</sub> with age for most cortical regions ( $p < 0.05$ ). Figure 3 shows the linear regressions for the two age intervals measured in the frontal region. Using the measured values for the change in CBV, SaO<sub>2</sub>, and StO<sub>2</sub> when statistically significant ( $p < 0.05$ ), and assuming a constant flow/volume relationship, we calculated regional CMRO<sub>2</sub> changes from 0 to 6 wk and from 12 to 50 wk. Table 1 summarizes the lack of change in CBV and CMRO<sub>2</sub> from 0 to 6 wk and the increase in CMRO<sub>2</sub> from 12 to 50 wk in the brain regions measured.

Grouping by region and across six target age groups [premature (<36 wk cGA), 0–2.5, 2.5–5, 5–6.5, 8–9.5, and 9.5–12 mo of age) identified regional variations in the timing of the HbT and CBV increases (see Fig. 4, *magenta vertical*

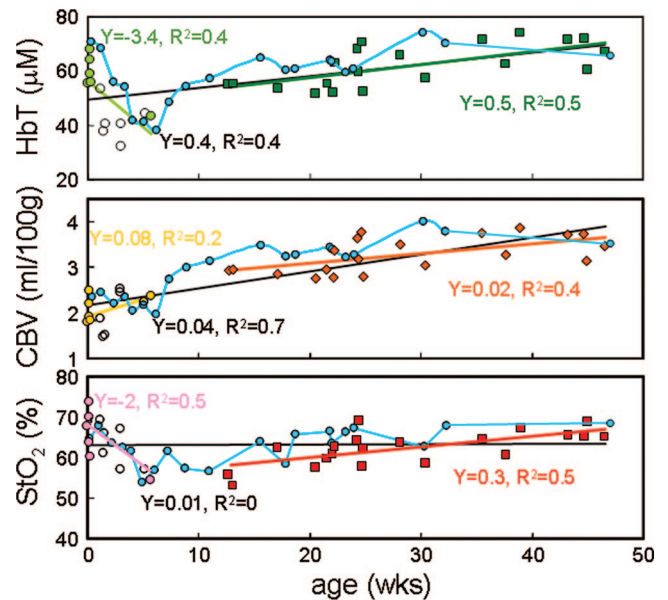


**Figure 3.** From top to bottom: HbT, CBV, and StO<sub>2</sub> as a function of age measured in the frontal region in all infants. The straight lines are the linear regressions from 0 to 6 wk, 12 to 50 wk, and 0 to 50 wk. The empty circles correspond to premature babies. The cyan circles are the results for a baby measured longitudinally 20 times from 0 to 11 mo. Y and  $R^2$  for each regression line are reported on the graphs with the same color as the regression line.

arrows,  $p < 0.05$ ). Figure 4 also shows the smaller variations of StO<sub>2</sub> with age in all brain regions, despite the large increases in HbT and CBV.

Finally, we measured one normal full-term baby 20 times over the course of the infant's first 11 mo. The longitudinal measurements of HbT, CBV, and StO<sub>2</sub> in the infant's frontal region (*cyan circles/lines* in Fig. 3) are within measurement error of the results from the cross-sectional analysis.

## DISCUSSION

Our results for HbT, CBV, and StO<sub>2</sub> in newborns agree with values reported in recent publications using frequency- and time-resolved systems (19,20). We extend the measurements to older infants and show that FD-NIRS provides quantitative measures of regional brain development by resolving region-specific changes in HbT, CBV, and StO<sub>2</sub> over the first year of life.

The measurements reported here demonstrate that it is not necessary to leave the probe in place for long periods of time, or to carefully reposition the probe on the exact location on the head; repeating measurement at few-minute intervals produced consistent results. By designing our system and protocol to provide abundant redundancy of data we can use systematic criteria to retain only the highest quality data sets to produce more accurate measures. The reproducibility of the measurements is within 5%, and the variability between same-age subjects for all parameters is smaller than the general variation across ages. Thus, the methodology can be easily used to learn more about brain development in healthy infants and, significantly, has potential for identifying where and at what rate deviations from normal development occur.

**Table 1.** HbT, CBV, and StO<sub>2</sub> at 0 and 6 wk, and 12 and 50 wk in six brain regions; CMRO<sub>2</sub> changes and p values for the regressions are also reported

	1 wk HGB = 17.3 g/dL			6 wk HGB = 12 g/dL			ΔCMRO <sub>2</sub>	p HbT	p CBV	p StO <sub>2</sub>
	HbT <sub>0</sub> (μM)	CBV <sub>0</sub> (mL/100 g)	StO <sub>20</sub> (%)	HbT (μM)	CBV (mL/100 g)	StO <sub>2</sub> (%)				
fr	53	2.0	66	36	2.4	56	0.91	2.E-02	1.E-01	4.E-03
oc	51	2.1	64	49	2.9	63	0.72	9.E-01	2.E-01	8.E-01
lt	51	1.9	68	26	1.8	52	1.04	9.E-03	9.E-01	1.E-02
lp	49	1.8	66	38	2.2	61	0.81	2.E-01	2.E-01	8.E-02
rt	50	1.9	68	37	2.4	59	0.89	3.E-02	5.E-02	5.E-04
rp	55	2.1	67	32	2.1	61	0.85	7.E-03	9.E-01	4.E-02
<b>avg</b>	<b>52</b>	<b>2.0</b>	<b>67</b>	<b>33</b>	<b>2.2</b>	<b>57</b>	<b>0.92</b>			
	12 wk HGB = 11.5 g/dL			52 wk HGB = 12 g/dL			ΔCMRO <sub>2</sub>	p HbT	p CBV	p StO <sub>2</sub>
	HbT <sub>0</sub> (μM)	CBV <sub>0</sub> (mL/100g)	StO <sub>20</sub> (%)	HbT (μM)	CBV (mL/100g)	StO <sub>2</sub> (%)				
fr	54	2.9	58	73	3.8	68	1.28	1.E-03	5.E-03	1.E-03
oc	64	3.5	64	82	4.2	65	1.50	3.E-02	8.E-02	8.E-01
lt	44	2.4	59	73	3.7	67	1.98	2.E-05	6.E-05	3.E-03
lp	53	2.9	61	70	3.6	70	1.21	2.E-02	4.E-02	1.E-03
rt	53	2.9	61	70	3.6	65	1.50	2.E-03	7.E-03	2.E-01
rp	51	2.8	61	73	3.8	67	1.59	7.E-03	3.E-02	2.E-02

The numbers in bold indicate statistical significance, with  $p < 0.05$ . fr, of, lt, lp, rt, rp.

Both across babies and in the longitudinal study we measured highly statistically significant increases in HbT and CBV with age for all cortical regions ( $p < 2E^{-4}$  and  $<4E^{-7}$ , respectively) corresponding to cerebral vascularization increases from birth to 1 y of age. FD-NIRS allows us to quantify tissue oxygenation as well as Hb concentration, and this measurement shows a new finding: StO<sub>2</sub> is relatively constant from birth to 1 y of age (see Figs. 3 and 4). The relatively minimal change in StO<sub>2</sub>, despite the marked increases in HbT, CBV, and CMRO<sub>2</sub>, may indicate that, in healthy infants, oxygen delivery to different brain regions and at different ages closely matches the local consumption. This result agrees with the hypothesis that increases in cerebral blood volume in different cortical regions occur in parallel and are tightly coupled with increases in the metabolic demand of neurons during development (35).

We hypothesize that the decrease in HbT and StO<sub>2</sub> from 0 to 6 wk is due to the large (40%) decrease in hematocrit during the physiological transition from fetal to adult Hb (25). The fact

that these decreases are constant across brain regions and the lack of change in CBV and CMRO<sub>2</sub> (Table 1) support this hypothesis. The relatively low constant CMRO<sub>2</sub> in the first 6 wk agrees with electrophysiological studies showing very low synaptic activity, SPECT studies showing low cortical blood flow, and FDG-PET studies showing low cortical glucose uptake in the first 2 mo (3,9). Thus, the low level of functional activity in the neonatal period results in minimal oxygen consumption and requires minimal blood flow. A gradual increase in basal cerebral artery flow velocity during the first 20 d of life of infants is reported in the literature (36). It is possible that the increase in blood flow during the initial postnatal period represents an attempt to maintain appropriate oxygenation, or flow increases simply because reduced HGB reduces blood viscosity and resistance, allowing flow to increase under constant pressure. In our measurements, we found that while the hematocrit and HbT decrease about 40%, StO<sub>2</sub> decreases only 20% from 0 to 6 wk. This smaller decrease in StO<sub>2</sub> is probably due to a blood flow increase. These measurements seem to indicate that flow and oxygenation are not perfectly coupled in the first weeks of life; further investigation is needed.

From 12 to 50 wk of age, hematocrit changes are negligible, with HGB increasing from 11.5 to 12 g/dL. We estimated CMRO<sub>2</sub> increases from 12 to 50 wk to be between 28 and 75% depending on the region (see Table 1). These increases in CMRO<sub>2</sub> closely follow the measured increases in CBV and the relatively constant StO<sub>2</sub>. The CMRO<sub>2</sub> increase is consistent with the increase in glucose metabolism observed by Chugani (3).

Figure 4 shows the regional difference in the timing of CBV increase. The first region to show a large increase in CBV is the occipital area. Here, CBV almost doubles in infants from 0–2.5 to 2.5–5 mo. At the same time, there is an increase in CBV in the parietal and temporal regions. In contrast, CBV in the frontal region increases more linearly, until it plateaus

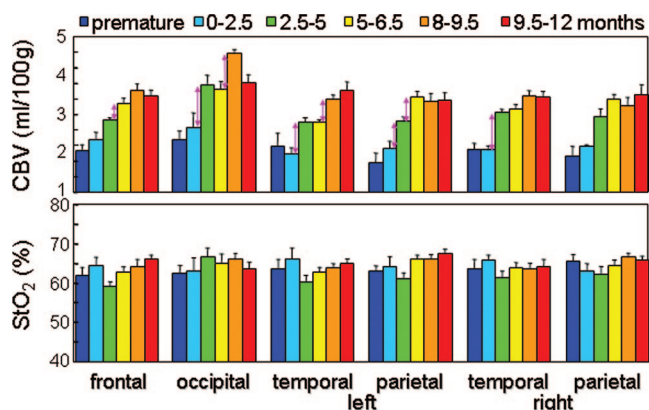


**Figure 4.** CBV and StO<sub>2</sub> for six age groups in the six brain regions. Magenta vertical arrows indicate  $p < 0.05$ . Error bars are standard errors between infants. The number of infants in each age group is 6, 8, 6, 7, 3, and 8, respectively.

between 8 and 9.5 mo. These regional differences in the evolution of CBV reveal the ages at which vasculature develops in different cortical regions. Our results are consistent with PET studies of glucose uptake (3), EEG studies (6), and developmental skill acquisition (4,5).

HbT, CBV, and StO<sub>2</sub> results for the longitudinal measurements are in agreement with those from the cross-sectional analysis. The reduced variability in the longitudinal data suggests that the larger variance observed in the cross-sectional data arises from intersubject variability. Similarly, in the group analysis, we found decreased variance within a subject at a given age compared with between subjects at the same age. Thus, performing longitudinal studies can confer greater statistical power. FD-NIRS is well suited for assessing brain development in at-risk infants using longitudinal measurements.

The results presented here are compelling and novel. More measurements are needed to increase the statistical significance of the data and to better define the timing and differentiate changes in all brain regions. Despite the small number of measurements (47 infants with an age range of 0–12 mo), our data reveal highly significant and regionally specific changes indicating the potential of this technique for investigating normal brain development in infants. The ability to safely monitor infants for regional cerebral development of oxygen utilization (CMRO<sub>2</sub>) and vascularization (CBV) at bedside may impact both clinical and behavioral brain studies.

**Acknowledgments.** The authors thank Pamela Almeida, Tina Chaves, Shalini Nadgir, Eleni Themelis, Teresa Wilcox, Eric Wruck, Weicheng Wu, and all the nurses in the NICU and Step Down clinics at MGH for the help and support with data collection. We also thank Gary Boas, Elizabeth Warren, and Sarah Barnett for helpful comments, and Theodore Huppert for assistance with data analysis. This work was also made possible through the inspiration and generous support of George Cowan.

## REFERENCES

- Kretschmann HJ, Kamradt G, Krauthausen I, Sauer B, Wingert F 1986 Brain growth in man. *Bibl Anat* 28:1–26
- Bourgeois JP, Rakic P 1993 Changes of synaptic density in the primary visual cortex of the macaque monkey from fetal to adult stage. *J Neurosci* 13:2801–2820
- Chugani HT, Phelps ME 1986 Maturation changes in cerebral function in infants determined by 18FDG positron emission tomography. *Science* 231:840–843
- Bayley N 1993 *The Bayley Scales of Infant and Toddler Development*. Psychological Corporation, New York
- Amiel-Tison C, Grenier A 1986 *Neurological Assessment during the First Year of Life*. Oxford University Press, New York
- Kellaway P 2003 Orderly approach to visual analysis: elements of the normal eeg, and their characteristics in children and adults. In: Ebersole JS, Pedley TA (eds) *Current Practice of Clinical Electroencephalography*, pp 100–159. Lippincott Williams & Wilkins, Philadelphia
- Chugani HT 1998 A critical period of brain development: studies of cerebral glucose utilization with PET. *Prev Med* 27:184–188
- Altman DI, Powers WJ, Perlman JM, Herscovitch P, Volpe SL, Volpe JJ 1988 Cerebral blood flow requirement for brain viability in newborn infants is lower than in adults. *Ann Neurol* 24:218–226
- Tokumaru AM, Barkovich AJ, O'Uchi T, Matsuo T, Kusano S 1999 The evolution of cerebral blood flow in the developing brain: evaluation with iodine-123 iodoamphetamine SPECT and correlation with MR imaging. *AJNR Am J Neuroradiol* 20:845–852
- Barkovich AJ, Kjos BO, Jackson DE Jr., Norman D 1988 Normal maturation of the neonatal and infant brain: MR imaging at 1.5 T. *Radiology* 166:173–180
- Mukherjee P, Miller JH, Shimony JS, Conturo TE, Lee BC, Almlí CR, McKinstry RC 2001 Normal brain maturation during childhood: developmental trends characterized with diffusion-tensor MR imaging. *Radiology* 221:349–358
- Peterson BS, Anderson AW, Ehrenkranz R, Staib LH, Tageldin M, Colson E, Gore JC, Duncan CC, Makuch R, Ment LR 2003 Regional brain volumes and their later neurodevelopmental correlates in term and preterm infants. *Pediatrics* 111:939–948
- Brazy JE, Lewis DV, Mitnick MH 1985 Noninvasive monitoring of cerebral oxygenation in preterm infants: preliminary observations. *Pediatrics* 75:217–225
- Wyatt JS, Cope M, Delpy DT, Wray S, Reynolds EO 1986 Quantification of cerebral oxygenation and haemodynamics in sick newborn infants by near infrared spectrophotometry. *Lancet* 2:1063–1066
- Benaron DA, Benitz WE, Ariagno RA, Stevenson DK 1992 Noninvasive methods for estimating *in vivo* oxygenation. *Clin Pediatr (Phila)* 31:258–273
- Nicklin SE, Hassan IA, Wickramasinghe YA, Spencer SA 2003 The light still shines, but not that brightly? The current status of perinatal near infrared spectroscopy. *Arch Dis Child Fetal Neonatal Ed* 88:F263–F268
- Benaron DA, Ho DC, Spilman S, Van Houten JP, Stevenson DK 1994 Tomographic time-of-flight optical imaging device. *Adv Exp Med Biol* 361:207–214
- Hebden JC, Gibson A, Yusof RM, Everdell N, Hillman EM, Delpy DT, Arridge SR, Austin T, Meek JH, Wyatt JS 2002 Three-dimensional optical tomography of the premature infant brain. *Phys Med Biol* 47:4155–4166
- Ijichi S, Kusaka T, Isobe K, Okubo K, Kawada K, Namba M, Okada H, Nishida T, Imai T, Itoh S 2005 Developmental changes of optical properties in neonates determined by near-infrared time-resolved spectroscopy. *Pediatr Res* 58:568–573
- Zhao J, Ding HS, Hou XL, Zhou CL, Chance B 2005 *In vivo* determination of the optical properties of infant brain using frequency-domain near-infrared spectroscopy. *J Biomed Opt* 10:024028.
- Fantini S, Franceschini MA, Maier JS, Walker SA, Barbieri B, Gratton E 1995 Frequency-domain multichannel optical detector for non-invasive tissue spectroscopy and oximetry. *Opt Eng* 34:32–42
- Franceschini MA, Fantini S, Paunescu LA, Maier JS, Gratton E 1998 Influence of a superficial layer in the quantitative spectroscopic study of strongly scattering media. *Appl Opt* 37:7447–7458
- Fabbri F, Sassaroli A, Henry ME, Fantini S 2004 Optical measurements of absorption changes in two-layered diffusive media. *Phys Med Biol* 49:1183–1201
- Wray S, Cope M, Delpy DT 1988 Characteristics of the near infrared absorption spectra of cytochrome aa3 and hemoglobin for the noninvasive monitoring of cerebral oxygenation. *Biochim Biophys Acta* 933:184–192
- Oski FA, Naiman JL 1982 *Hematologic problems in the newborn*, 3rd Ed. Major Probl Clin Pediatr 4:1–360
- Watzman HM, Kurth CD, Montenegro LM, Rome J, Steven JM, Nicolson SC 2000 Arterial and venous contributions to near-infrared cerebral oximetry. *Anesthesiology* 93:947–953
- Grubb RL, Phelps ME, Eichling JO 1974 The effects of vascular changes in PaCO<sub>2</sub> on cerebral blood volume, blood flow, and vascular mean transit time. *Stroke* 5:630–639
- Brown DW, Hadway J, Lee TY 2003 Near-infrared spectroscopy measurement of oxygen extraction fraction and cerebral metabolic rate of oxygen in newborn piglets. *Pediatr Res* 54:861–867
- Stegink LD, Meyer PD, Brummel MC 1971 Human fetal hemoglobin F I. Acetylation status. *J Biol Chem* 246:3001–3007
- Wolthuis R, van Aken M, Fountas K, Robinson JS, Jr Bruining HA, Puppels GJ 2001 Determination of water concentration in brain tissue by Raman spectroscopy. *Anal Chem* 73:3915–3920
- Zijlstra WG, Buursma A, Meeuwse-van der Roest WP 1991 Absorption spectra of human fetal and adult oxyhemoglobin, de-oxyhemoglobin, carboxyhemoglobin, and methemoglobin. *Clin Chem* 37:1633–1638
- Wyatt JS, Cope M, Delpy DT, Richardson CE, Edwards AD, Wray S, Reynolds EO 1990 Quantitation of cerebral blood volume in human infants by near-infrared spectroscopy. *J Appl Physiol* 68:1086–1091
- Lammertsma AA, Brooks DJ, Beaney RP, Turton DR, Kensett MJ, Heather JD, Marshall J, Jones T 1984 *In vivo* measurement of regional cerebral haematocrit using positron emission tomography. *J Cereb Blood Flow Metab* 4:317–322
- Okazawa H, Yonekura Y, Fujibayashi Y, Yamauchi H, Ishizu K, Nishizawa S, Magata Y, Tamaki N, Fukuyama H, Yokoyama A, Konishi J 1996 Measurement of regional cerebral plasma pool and hematocrit with copper-62-labeled HSA-DTS. *J Nucl Med* 37:1080–1085
- Tieman SB, Mollers S, Tieman DG, White J 2004 The blood supply of the cat's visual cortex and its postnatal development. *Brain Res* 998:100–112
- Bode H, Wais U 1988 Age dependence of flow velocities in basal cerebral arteries. *Arch Dis Child* 63:606–611